J Appl Electrochem (2010) 40:865–873
DOI 10.1007/s10800-009-0062-5

ORIGINAL PAPER

Electrochemical copolymerization and characterization of dianilines linked by polyether bridge with aniline

Seha Tirkeş · Ahmet M. Önal

Received: 14 August 2009 / Accepted: 26 December 2009 / Published online: 13 January 2010

Abstract Copolymer of aniline and triethylene glycol *bis*(*o*-aminophenyl) ether was synthesized by constant potential electrolysis. Cyclic voltammogram of the copolymer films recorded in the monomer-free electrolytic solution revealed that the redox behavior of the films approaches to that of poly(triethylene glycol *bis*(*o*-aminophenyl) ether) with increasing amount of triethylene glycol *bis*(*o*-aminophenyl) in the feed ratio. Copolymerization was investigated by in situ recording the changes in the electronic absorption spectrum during electrolysis. The free standing copolymer film was characterized utilizing Fourier transform infrared spectrometer, and spectroelectrochemical behavior of the copolymer was investigated via in situ UV–vis spectroscopic technique. Besides the electron spin resonance study of the copolymer film, the different morphologies of the polymers were examined by scanning electron microscopy and the copolymerization was confirmed. The temperature dependence conductivity of the copolymer film was measured by four-probe technique in the temperature range of 100–300 K, and the calculated parameters showed that conduction mechanism fits to variable range hopping.

Keywords Copolymer · Polyether bridge · Polyaniline · Variable range hopping

S. Tirkeş
Chemistry Group, Faculty of Engineering, Atılım University, İncek, 06836 Ankara, Turkey

A. M. Önal (✉)
Department of Chemistry, Middle East Technical University, İnönü Bulvari, 06531 Ankara, Turkey
e-mail: aonal@metu.edu.tr

1 Introduction

The development of organic π-conjugated polymers has been intensively pursued because they have a great potential for advanced technological applications in the field of photovoltaics [1–5], transistors [6–9], light emitting diodes [10–13], and molecular electronics [14–16]. Particularly, they have become one of the most favored electrochromes in optical displays [17], smart windows [18, 19], devices [20, 21], mirrors [22, 23], and camouflage materials [24, 25] because of their low cost, compatibility, and tunable intrinsic properties (electronic, optical, conductivity, and stability) offered by the structural design of the starting materials [26–28]. However, their poor processibility and solubility restrict their common use. To overcome these drawbacks, one way is to functionalize the monomer prior to polymerization or to copolymerize it with other monomers.

Copolymerization leads materials with intermediate properties between two homopolymers, thus allowing modification of the physical properties of conducting polymers. Among conducting polymers, polyaniline (PANI) is unique not only because of its stability in air but also its solubility in some solvents which enhances processibility. However, there are also studies involving its copolymerization or functionalization to alter its properties. The copolymerization of aniline (ANI) with *o*-, *m*-, and *p*-phenylenediamines [29], *o*-toluidine [30], and *o*-methoxyaniline [31] are the examples of studies where the objectives are to control the electrical conductivity and/or examine the effect of monomer feed ratio on electrical conductivity. The copolymerization of ANI with thiophene and the increase in the conductivity with increasing thiophene concentration were also investigated [32]. Furthermore, electrochemical copolymerization of ANI with aniline-2,5-disulfonic acid [33],

o-aminobenzonitrile [34], *m*-phenylenediamine [35], *N*-butylaniline [36], and *o*-toluidine [36, 37] are the examples of efforts to improve the properties of PANI. The copolymerization of *o*-aminophenol with ANI was studied by in situ spectroelectrochemical method in a detailed manner [38]. Besides the aniline copolymerization, *o*- and *m*-methoxyaniline were copolymerized with diphenylamine and investigated via UV–vis technique [39, 40] as well. Although there are large number of examples of functionalized monomers substituted with crown ethers and/or polyether chains in order to design modified electrodes for electrochemical and bioelectrochemical sensors which can provide an electrical transduction of ionic information [41–46], there are only few reports on the polymerization of polyether substituted ANI derivatives [47–49].

In this connection, recently, we have studied electrochemical polymerization of triethylene glycol *bis*(*o*-aminophenyl) ether (**I**) and found that the corresponding polymer film **PI** can be reversibly cycled between its neutral and oxidized states; however, it exhibited relatively lower conductivity as compared to PANI [50]. Taking into account these results, we turned our attention to a new copolymer of aniline. In this article, we wish to report the synthesis of copolymer bearing pseudo-polyether cages with reasonable conductivity to be amenable for use in sensors. The copolymerization of **I** with ANI monomer was investigated and the copolymer was characterized in terms of cyclic voltammetry (CV), Fourier transform infrared (FTIR) spectrometer, and in situ UV–vis spectroscopic techniques. Furthermore, the results of conductivity measurements in the temperature range of 100–300 K were also represented.

2 Experimental details

2.1 Materials

The synthesis of **I** was achieved according to the procedure described in the literature [51]. Electrochemical polymerization of **I** was already explained in a previous work [50]. ANI monomer was purchased from Merck and used after distillation. The copolymerization of **I** and ANI was achieved in 3.0 M H_2SO_4 aqueous solution by applying CV and constant potential electrolysis techniques. Since the synthesis of freestanding polymer films could only be achieved in water with high acid concentration [50] the same medium was used also for copolymerization studies. The synthesized polymer was dried under vacuum at room temperature for 72 h.

2.2 Measurements

Electrochemical measurements were made using a Gamry potentiostat (equipped with PHE 200 Physical electrochemistry software). During CV studies, glassy carbon, Pt, and Ag/AgCl were used as working, counter, and reference electrodes, respectively. For spectroelectrochemical studies, platinum and silver wires were used as counter and reference electrodes, respectively. An indium-tin-oxide-coated electrode (ITO, Delta Tech. 8–12 Ω, 0.7 cm × 5 cm) was used as the working electrode. Electrolytic solution (3.0 M H_2SO_4 (aq)) was purged with Ar(g) for 30 min prior to spectroelectrochemical studies, and the measurements were done under Ar(g) atmosphere using a HP 8453A diode array UV–visible spectrometer. FTIR spectra of the samples were recorded using a Bruker Vertex-70 FTIR spectrophotometer. The morphologies of copolymer films and PANI deposits were examined utilizing FEI Quanta 400 scanning electron microscope. Varian E12 ESR spectrometer operating at X-band with 100 kHz field modulation was used for investigating paramagnetic behavior of the polymers at room temperature.

The dc conductivity measurements were done by four-probe technique at about 10^{-5} atm. Constant current was applied to the samples by using a Keithley 6220 programmable current source, and the voltage changes were measured by a Keithley 6514 electrometer. The temperature dependent conductivity between 100 and 300 K was studied in Janis cryostat, and the temperature was adjusted by using Lake Shore 331 temperature controller unit.

3 Results and discussions

3.1 Voltammetric studies of mixture of I and ANI

Since the oxidation potential values of both monomers, **I** and ANI, are the same [50], oxidation of monomer mixtures can form copolymers due to competing reactions between them during electrolysis. Therefore, the cyclic voltammograms of ANI solution and ANI/**I** mixtures with three different ratios were recorded in the potential range of 0.0–1.3 V and the results obtained during first 20 cycles are depicted in Fig. 1. The cyclic voltammogram of ANI in concentrated H_2SO_4 (3.0 M) is different from its well known voltammogram (Fig. 1a). As seen in Fig. 1c, three reversible peaks started to intensify at about 0.30, 0.42 and 0.60 V after the first anodic scan representing the ANI incorporation. Furthermore, redox behavior of the copolymer film approached to that of **PI** with increasing amount of **I** in the monomer mixture (Fig. 1g) which is further evidenced by recording the cyclic voltammogram of polymer films in monomer-free electrolyte solutions (see Fig. 1b, d, f, h).In this work, a feed ratio of 10:2 (ANI/**I**) was selected for detailed investigation of copolymer.

The electronic absorption spectra of **I**, ANI, and ANI/**I** mixture recorded during electrolysis at 1.2 V versus Ag

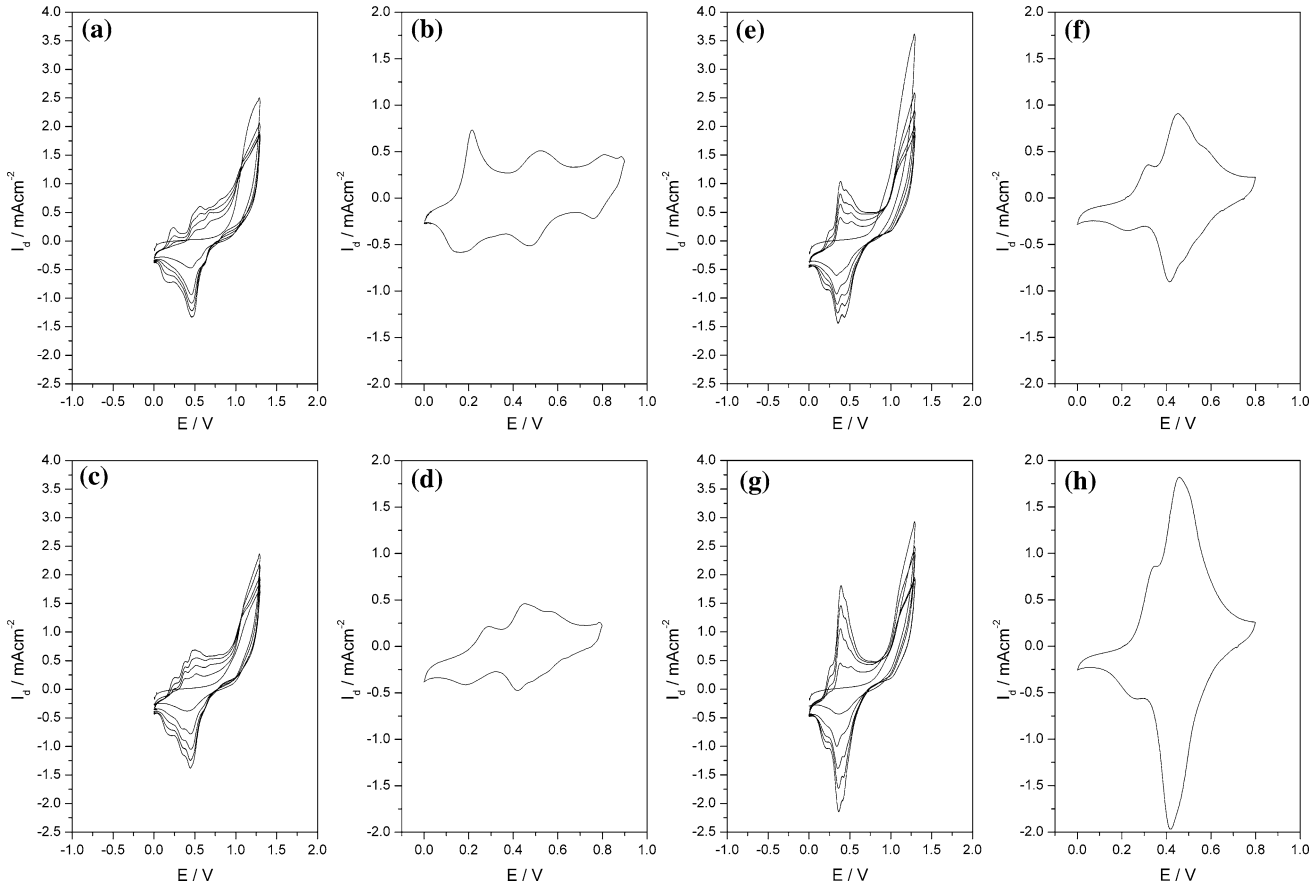

Fig. 1 Repetitive cycles of **a** ANI, and ANI/**I** with different compositions; **c** 10/1 (40.0 mM/4.0 mM), **e** 10/2 (40.0 mM/8.0 mM), **g** 10/5 (40.0 mM/20.0 mM), and CV of **b** PANI, and poly(**I**-co-ANI) synthesized from different compositions; **d** 10/1 (40.0 mM/4.0 mM), **f** 10/2 (40.0 mM/8.0 mM), **h** 10/5 (40.0 mM/20.0 mM)

wire are depicted in Fig. 2. First of all, upon starting electrolysis of **I** a new band at about 475 nm started to intensify immediately with a concomitant increase in 360 nm band which is most probably due to π–π^* transition within leucoemeraldine form [52]. Since the absorption band at 475 nm diminished after stopping the electrolysis, this band was ascribed to absorption of an intermediate [38]. For the sake of comparison, the electronic absorption spectrum of ANI solution was also monitored throughout the electrolysis (Fig. 2b). In the spectrum of ANI two absorption bands (360 and 710 nm) were observed. The band at 360 nm can be attributed to π–π^* transition of benzonoid rings, characteristic for the leucoemeraldine form of PANI, and the latter can be ascribed to *N*-phenyl-*p*-phenylenediamine dimers and its dications [38]. The changes in the electronic absorption spectrum recorded during the constant potential electrolysis of ANI/**I** mixture, however, exhibit similarities with that **I** as expected (Fig. 2c). The absorption bands at approximately 365 and 490 nm are almost at the same wavelength as that of **I**. On the other hand, the broad band centered at about 740 nm reveals the incorporation of ANI units bearing conjugation. It is noteworthy to mention that while constant potential electrolysis of ANI yields PANI in the powder form, the free standing film was formed only from the ANI/**I** mixture. The insertion of polyetheric chains between ANI units may be the reason for film formation even at low concentrations.

3.2 Structure and morphology analysis of poly(I-co-ANI)

For the morphological comparison, copolymer was synthesized by electrolysis at 1.2 V versus Ag wire on ITO from the ANI/**I** (10/2) mixture. The film form of copolymer and **PI** and the powder form of PANI were inspected by using SEM (Fig. 3). Contrary to smooth and uniform surface of **PI** (Fig. 3b, e) or the fibrillar surface of PANI (Fig. 3a, d), the copolymer film has a coarse surface (Fig. 3c, f) indicating a new feature between two homopolymers.

In order to find supplementary evidences for the copolymer formation, the ESR spectra of **PI** and copolymer were recorded (Fig. 4). Although the spectra are similar in

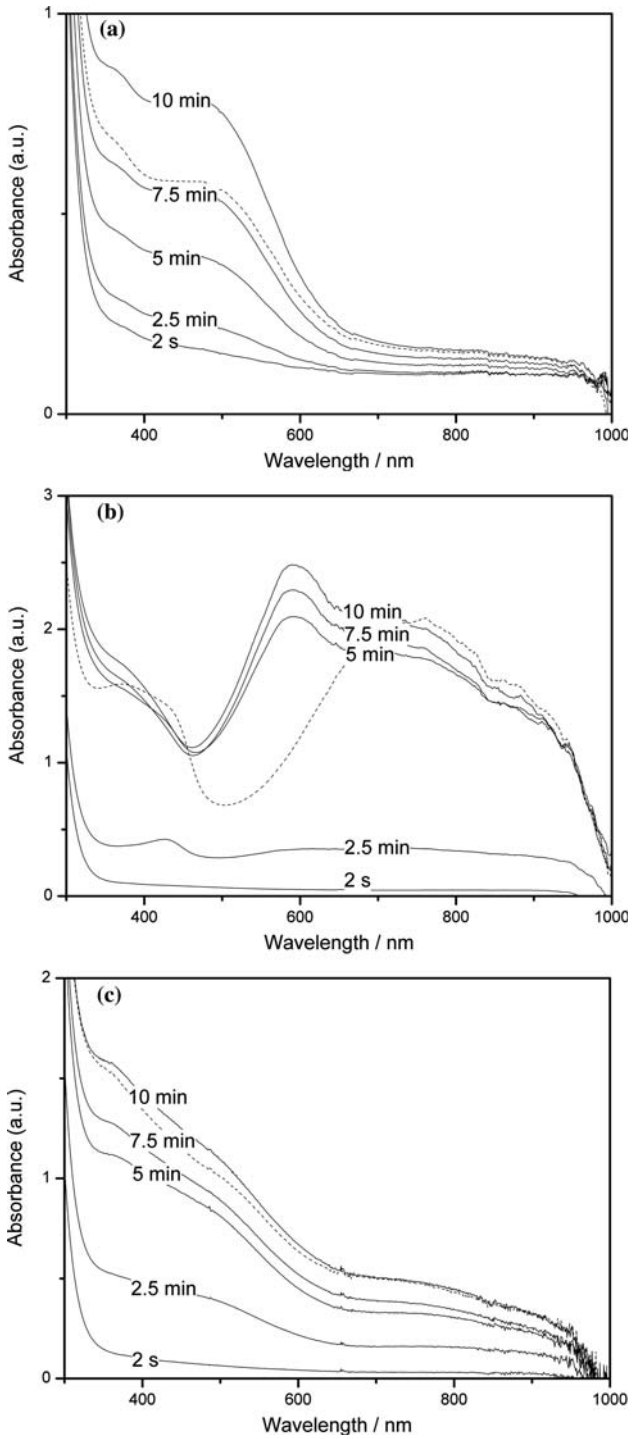

Fig. 2 Changes in the electronic absorption spectra recorded during the polymerization of **a** 8.0 mM **I**, **b** 40.0 mM ANI, and **c** ANI/**I** (40.0 mM/8.0 mM) monomer mixture. *Dashed lines* show the spectra recorded 2.5 min after switching off the potential

appearance with g value close to that of free electron and all in Dysonian shape, the line widths, ΔH_{pp}, were found to be 1.9 and 0.8 mT for **PI** and poly(**I**-co-ANI), respectively. The lower ΔH_{pp} value in the case of poly(**I**-co-ANI) indicates higher charge carrier mobility than that of **PI** [53]. Additionally, the asymmetry factor, A/B, of the asymmetric Dysonian shaped lines were found to increase from 1.5 for **PI** to 3.1 for poly(**I**-co-ANI). This type of line shape is characteristic for highly doped polymers and indicates an increased interaction of charge carriers within the skin with microwave field [54]. Thus, the increase in the A/B ratio is not only a further evidence for the copolymer formation but also indicates the enhancement of conductivity [55]. This result is also consistent with the room temperature conductivity measurements. The room temperature conductivity of poly(**I**-co-ANI) was found to be one order of magnitude greater (1.1×10^{-2} S cm^{-1}) than that of **PI** [50]. Furthermore, FTIR spectra of poly (**I**-co-ANI)) (Fig. 5) was also recorded to confirm the presence of polyether bridges along the copolymer backbone. The band at about 3,220 cm^{-1} indicates that the electrochemical polymerization takes place via $-NH_2$ groups. The bands at 1,490 and 1,575 cm^{-1} correspond to quinoid and benzenoid structures of copolymer film. The peaks at about 748 and 810 cm^{-1} are associated with *o*- and *p*-substitution in the polymer backbone, indicating the presence of two adjacent hydrogen atoms. In addition, the presence of aliphatic $-CH_2$ bands around 2,870 cm^{-1}, and –C–O–C– bands around 1,100 cm^{-1} in the FTIR spectrum of copolymer confirms the existence of polyether bridges in copolymer backbone. Under the light of these findings, the mechanism for copolymerization and a plausible structure for poly(**I**-co-ANI) are given in Scheme 1 and 2, respectively.

3.3 Spectroelectrochemical behavior

To reveal the electro-optical properties of the copolymer, the copolymer film was coated on ITO at a constant potential of 1.2 V and optoelectrochemical spectra were recorded in the monomer-free electrolyte solution. The in situ absorption spectra of PANI at various applied potentials between −0.2 and 0.5 V were recorded as well (Fig. 6, *inset*). The absorption around 295 nm in spectrum of PANI in neutral state can be attributed to the π–π^* transition of benzenoid rings of the leucoemeraldine form of the polymer [56]. The band at around 435 nm as observed also in **PI** can be ascribed to radical cation intermediates [50, 57]. It is worth noting that in spectra of both PANI and poly(**I**-co-ANI) (Fig. 6) there is a blue shift for the absorption band at around 700 nm with increasing potential indicating a transition from leucoemeraldine form to emeraldine form [56]. These shifts may occur due to the conformational changes during doping/dedoping process of PANI [58] and poly(**I**-co-ANI). Such conformational changes described as compact coil or extended coil transitions altering the absorption spectra [59, 60]. The E_g

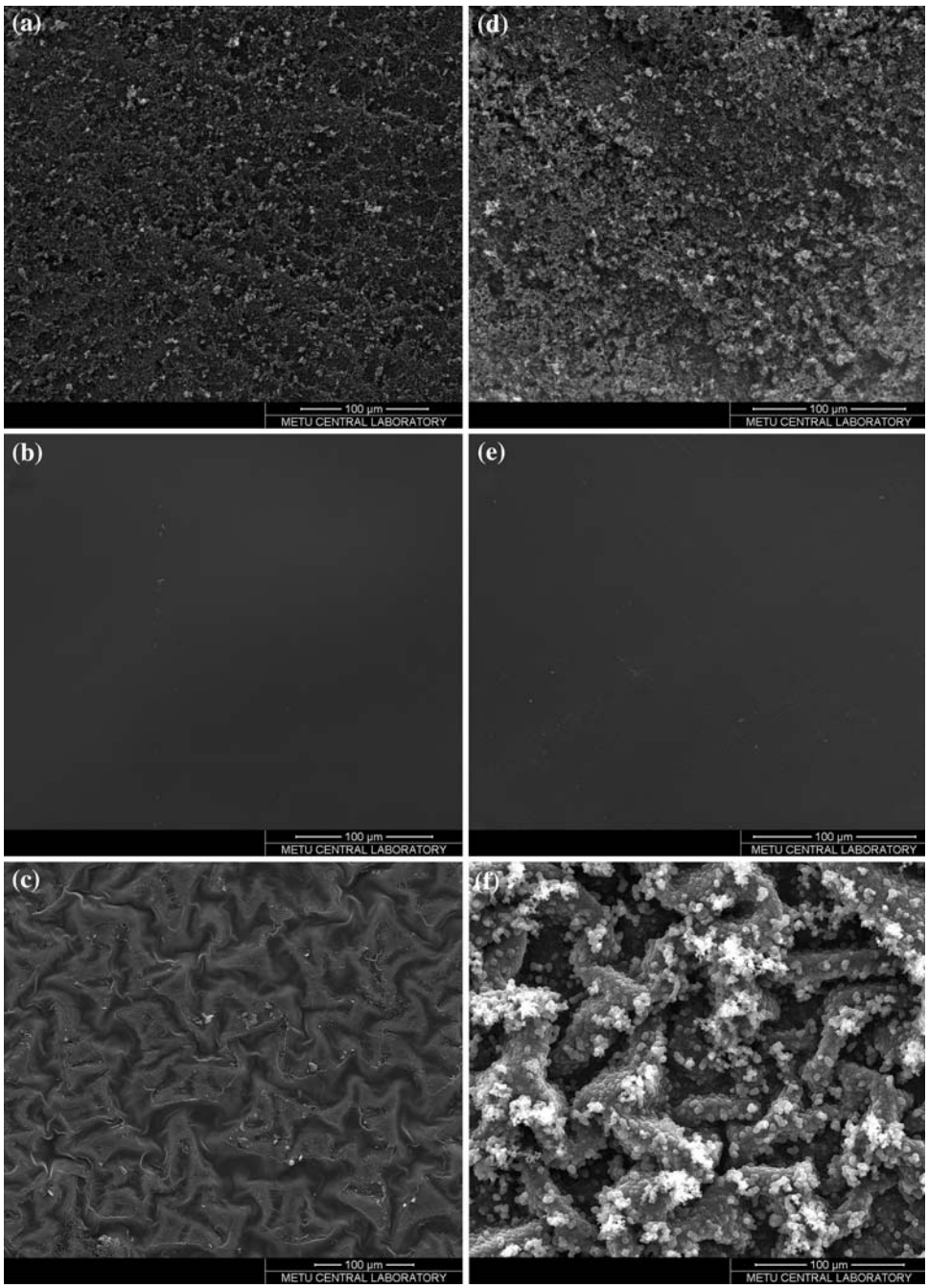

Fig. 3 Scanning electron micrographs: electrode side of **a** PANI, **b PI**, **c** poly(**I**-co-ANI), and solution side of **d** PANI, **e PI**, **f** poly(**I**-co-ANI)

values of PANI and poly(**I**-co-ANI) were found to be 2.71 and 3.01 eV, respectively, by the commencement on the lower energy end of π–π^* transitions [61]. The difference might be due to the insertion of **I** into ANI units which caused an increase in the band gap of PANI.

3.4 Temperature dependent conductivity of poly(I-co-ANI)

In order to investigate the temperature dependence of conductivity of the poly(**I**-co-ANI), the changes in conductivity versus temperature were analyzed by following relation [62].

$$\sigma = \sigma_0 \exp\left(\frac{-E_a}{T}\right). \quad (1)$$

The conductivity–temperature profile of the poly(**I**-co-ANI) (Fig. 7, *inset*) has two linear regions below and above 175 K. The slopes of these regions correspond to activation energies of 25.5 and 39.6 meV for the temperatures lower and higher than 175 K, respectively. This result reveals that the $\ln(\sigma)$-T^{-1} behavior is nonlinear in the given temperature interval.

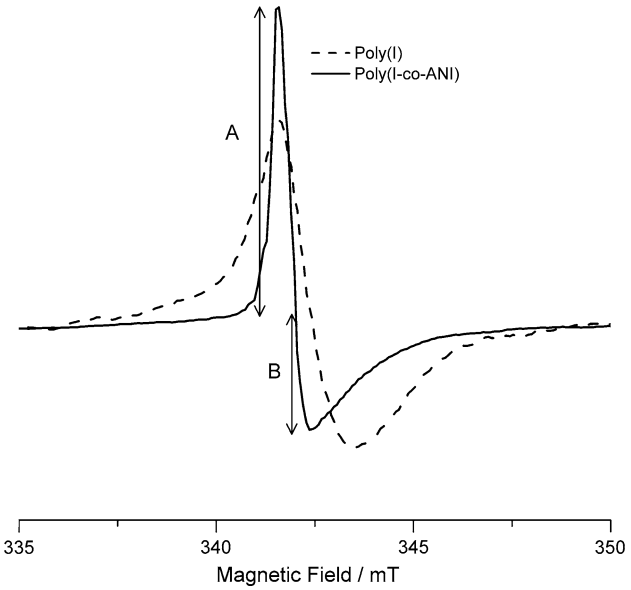

Fig. 4 ESR spectra of **PI** and poly(**I**-co-ANI) recorded at room temperature, field setting 336 T and microwave power 5 mW

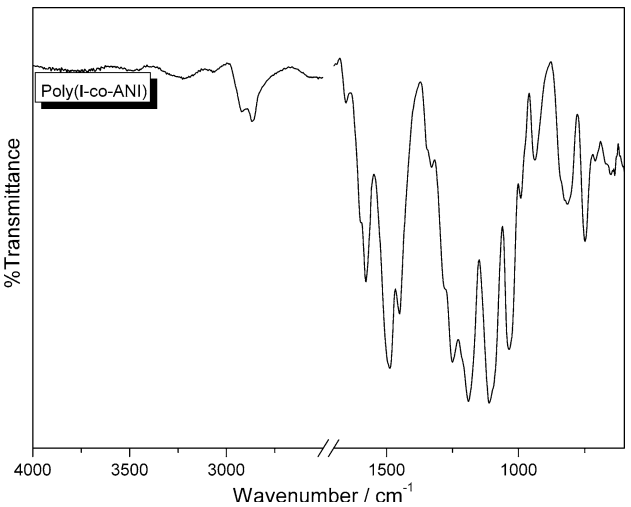

Fig. 5 FTIR spectrum of poly(**I**-co-ANI)

The results were also analyzed according to Mott's variable range hopping (VRH) model [63]. The following expression was used for the temperature dependent conductivity,

$$\sigma = \sigma_0 \exp\left(-\left(\frac{T_0}{T}\right)^{\frac{1}{d+1}}\right) \quad (2)$$

where d is dimensionality 1, 2, or 3.

In order to estimate the dimensionality of the hopping process the plots of $\ln(\sigma)$ versus $T^{-1/2}$, $\ln(\sigma)$ versus $T^{-1/3}$, and $\ln(\sigma)$ versus $T^{-1/4}$ were obtained. Among the three plots, the most linear behavior was found in three dimensions with a regression coefficient of 0.9994 (Fig. 7) for the copolymer. Similar results at given temperature interval were also reported for doped poly(*o*-methoxyaniline) [58] and PANI [64, 65].

Although the obtained plot was linear, the Mott's parameters were also calculated in order to check the Mott's requirements by using following equations.

$$T_0 = \frac{\lambda\alpha^3}{k_B N(E_F)} \quad (3)$$

$$\sigma_0 = e^2 \upsilon R^2 N(E_F) \quad (4)$$

where σ_0 is the pre-exponential factor and T_0 is the characteristic temperature found from the intercept and slope of $\ln(\sigma)$ versus $T^{-1/4}$, respectively. λ is the dimensionless constant (≈ 18.1) [66], e is the electronic charge, α is the coefficient of exponential decay of the localized states, the characteristic phonon frequency υ is $\approx 10^{13}$ Hz [67], k is the Boltzmann's constant, and $N(E_F)$ is the density of localized states at the Fermi level. The definition of the average hopping distance, R, and the average hopping energy, W, are as follows.

$$R = \{9/[8\pi\alpha k_B T N(E_F)]\}^{1/4} \quad (5)$$

$$W = 3/\left[4\pi R^3 N(E_F)\right]. \quad (6)$$

The calculated values of T_0 (8.63×10^5 K) and σ_0 (17.86 S cm^{-1}) were substituted into Eqs. 4 and 5 in order to obtain α and $N(E_F)$, which were found as 0.0496×10^8 cm^{-1} and 2.96×10^{19} cm^{-3} eV^{-1}, respectively. In addition, the values of R (61.3 Å) and W (35.0 meV) were calculated by using Eqs. 5 and 6.

Based on foregoing results, it can be safely concluded that the temperature dependent conductivity of poly(**I**-co-ANI) between 100 and 300 K is explained by VRH mechanism in three dimensions and the calculated parameters are consistent with Mott's requirements that are $\alpha R \gg 1$ and $W \gg kT$.

4 Conclusions

In summary, the copolymer of **I** and ANI was synthesized in the form of a free standing film by both potentiodynamic and potentiostatic methods. The copolymer was investigated by spectroscopic methods, and the FTIR results showed that the polyether bridge in **I** was protected during copolymerization. The expected morphological differences, confirming copolymerization, between homopolymers and copolymer were seen by SEM. The combination of **I** and ANI in the copolymer caused increase in room temperature conductivity relative to that

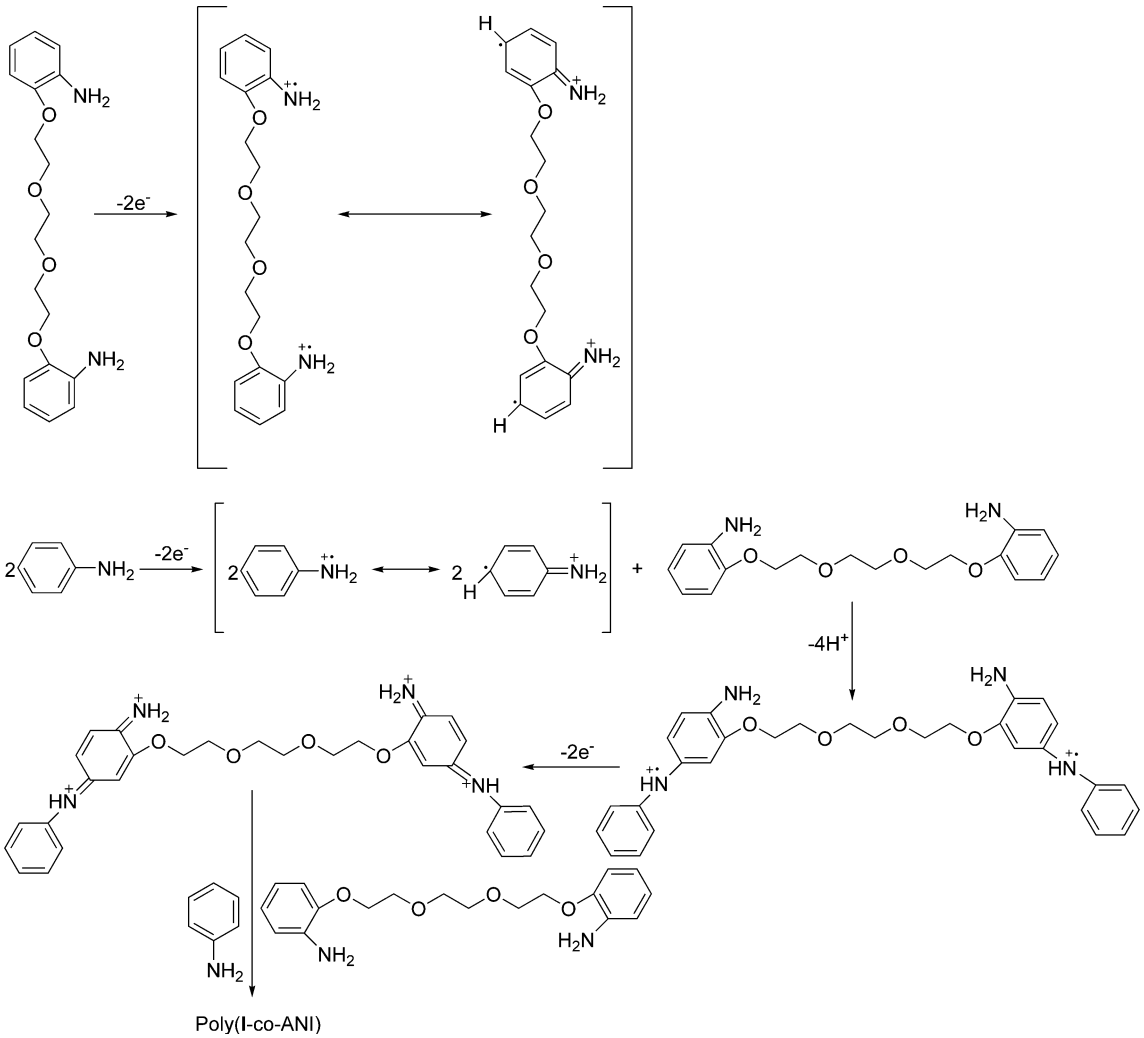

Scheme 1 Copolymerization of aniline with **I**

Scheme 2 A plausible structure for poly(**I**-co-ANI)

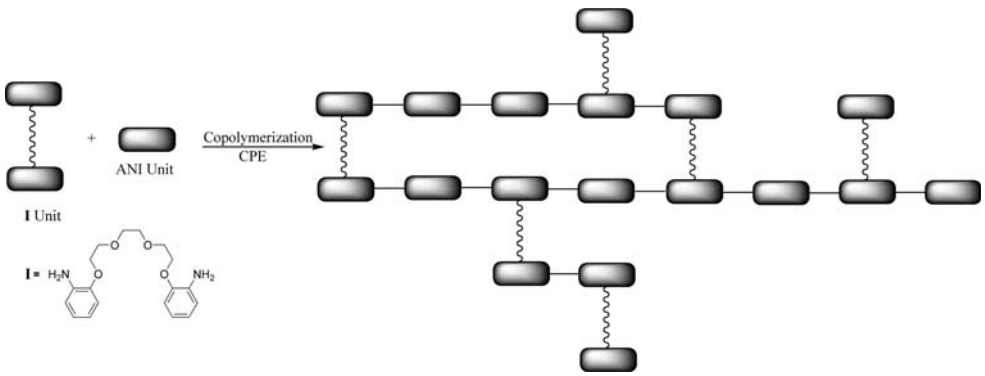

of **PI**. Furthermore, the conduction mechanism of the copolymer was elucidated by measurements of temperature dependent conductivity. The obtained data showed that the Mott's requirements in three dimensions were satisfied. The obtained conductive copolymer with pseudo-polyether cages represents a promising candidate to utilize as a sensor material. Work in this line is in progress.

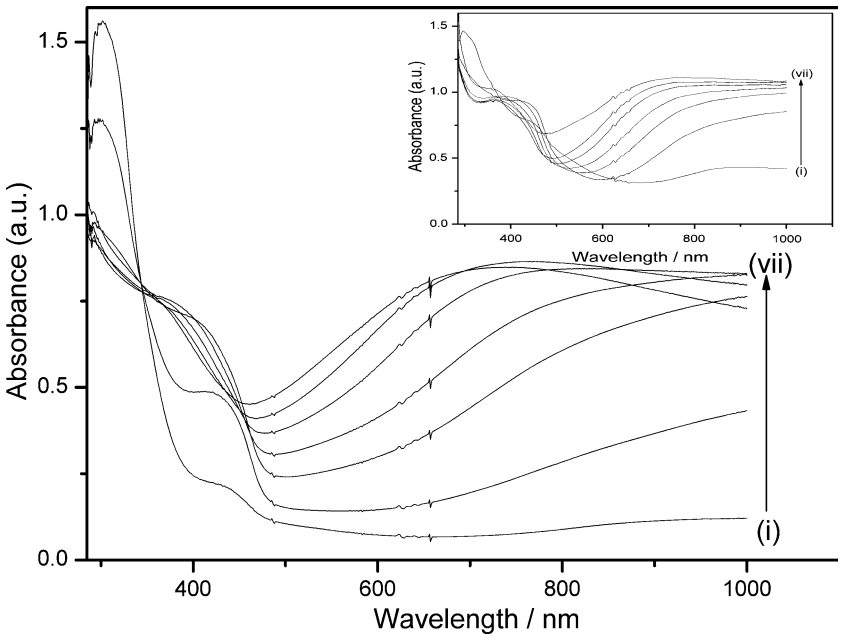

Fig. 6 Electronic absorption spectra of poly(**I**-co-ANI) synthesized from (ANI/**I**; 10/2; 40.0 mM/8.0 mM), *inset*: electronic absorption spectra of PANI in aqueous solution of 3.0 mol L^{-1} H_2SO_4 obtained at (*i*) −0.2 V, (*ii*) 0.0 V, (*iii*) 0.1 V, (*iv*) 0.2 V, (*v*) 0.3 V, (*vi*) 0.4 V, and (*vii*) 0.5 V

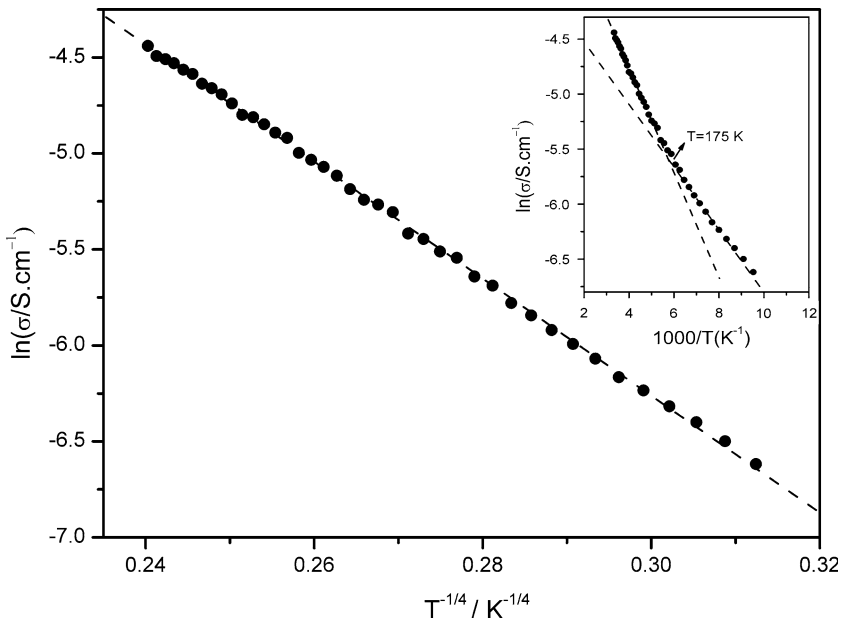

Fig. 7 The dc conductivity changes of poly(**I**-co-ANI) as a function of $T^{-1/4}$, *inset*: temperature dependence of dc conductivity of poly(**I**-co-ANI)

Acknowledgment The authors express their gratitude to Scientific and Technical Research Council of Turkey (TUBITAK) Project No. 104T423 for financial support.

References

1. Schmidt-Mende L, Fechtenkötter A, Müllen K, Moons E, Friend RH, MacKenzie JD (2001) Science 293:1119
2. Liscio A, De Luca G, Nolde F, Palermo V, Müllen K, Samori P (2008) J Am Chem Soc 130:780
3. Thompson BC, Fréchet JMJ (2008) Angew Chem Int Ed 7:58
4. Dance ZEX, Ahrens MJ, Vega AM, Ricks AB, McCamant DW, Ratner MA, Wasielewski MR (2008) J Am Chem Soc 130:83
5. Hagberg DP, Yum J-H, Lee H, De Angelis F, Marinado T, Karlsson KM, Humphry-Baker R, Sun L, Hagfeldt A, Grätzel M, Nazeeruddin Md K (2008) J Am Chem Soc 130:6259
6. Muccini M (2006) Nat Mater 5:605
7. Gao P, Beckmann D, Tsao HN, Feng X, Enkelmann V, Pisula W, Müllen K (2008) Chem Commun 13:1548
8. Usta H, Facchetti A, Marks TJ (2008) J Am Chem Soc 130:8580
9. Yang C, Kim JY, Cho S, Lee JK, Heeger AJ, Wudl F (2008) J Am Chem Soc 130:6444
10. Greenham NC, Moratti SC, Bradley DDC, Friend RH, Holmes AB (1993) Nature 365:628
11. Friend RH, Gymer RW, Holmes AB, Burroughes JH, Marks RN, Taliani C, Bradley DDC, Dos Santos DA, Bredas JL, Lögdlund M, Salaneck WR (1999) Nature 397:121
12. List EJW, Guentner R, De Freitas PS, Scherf U (2002) Adv Mater 14:374

13. Goel A, Dixit M, Chaurasia S, Kumar A, Raghunandan R, Maulik PR, Anand RS (2008) Org Lett 10:2553
14. Palma M, Levin J, Lemaur V, Liscio A, Palermo V, Cornil J, Geerts Y, Lehmann M, Samori P (2006) Adv Mater 18:3313
15. Chen X, Jeon Y-M, Jang J-W, Qin L, Huo F, Wei W, Mirkin CA (2008) J Am Chem Soc 130:8166
16. Coi T-L, Lee K-H, Joo W-J, Lee S, Lee T-W, Chae MY (2007) J Am Chem Soc 129:9842
17. Bange K, Gambke T (1990) Adv Mater 2:10
18. Pennisi A, Simone F, Barletta G, Di Marco G, Lanza L (1999) Electrochim Acta 44:3237
19. Rauh RD (1999) Electrochim Acta 44:3165
20. Schwendeman I, Hickman R, Sonmez G, Schottland P, Zong K, Welsh DM, Reynolds JR (2002) Chem Mater 14:3118
21. Meng H, Tucker D, Chaffins S, Chen Y, Helgeson R, Dunn B, Wudl F (2003) Adv Mater 15:146
22. Mortimer RJ (1997) Chem Soc Rev 26:147
23. Rosseinsky DR, Mortimer RJ (2001) Adv Mater 13:783
24. Chandrasekhar P, Zay BJ, Birur GC, Rawal S, Pierson EA, Kauder L, Swanson T (2002) Adv Funct Mater 12:95
25. Beaupré S, Breton A-C, Dumas J, Leclerc M (2009) Chem Mater 21:1504
26. Skotheim TA, Reynolds JR (eds) (2007) Handbook of conducting polymers-conjugated polymers: synthesis, properties and characterization. CRC Press, Boca Raton
27. Forrest SR (2004) Nature 428:911
28. Reese C, Roberts M, Ling M-M, Bao Z (2004) Mater Today 7:20
29. Prokeš J, Stejskal J, Křivka I, Tobolková E (1999) Synth Met 102:1205
30. Wei Y, Hariharan R, Patel SA (1990) Macromolecules 23:758
31. Motheo AJ, Pantoja MF, Venancio EC (2004) Solid State Ion 171:91
32. Udum YA, Pekmez K, Yildiz A (2005) Eur Polym J 41:1136
33. Tang H, Kitani A, Ito S (1997) Electrochim Acta 42:3421
34. Sato M, Yamanaka S, Nakaya JI, Hyodo K (1994) Electrochim Acta 39:2159
35. Mazeikiene R, Malinauskas A (1998) Synth Met 92:259
36. Ye S, Do NT, Dao LH, Vijh AK (1997) Synth Met 88:65
37. Kumar D (2000) Synth Met 114:369
38. Shah AA, Holze R (2006) Synth Met 156:566
39. Thanneermalai M, Jeyaraman T, Sivakumar C, Gopalan A, Vasudevan T, Wen TC (2003) Spectrochim Acta A 59:1937
40. Santhosh P, Gopalan A, Vasudevan T (2003) Spectrochim Acta A 59:1427
41. Goldenberg LM, Bryce MR, Petty MC (1999) J Mater Chem 9:1957
42. Bäuerle P, Scheib St (1995) Acta Polym 46:124–129
43. Marsella MJ, Carroll PJ, Swager TM (1995) J Am Chem Soc 117:9832–9841
44. Roncali J (1992) Chem Rev 92:711
45. Higgins SJ (1997) Chem Soc Rev 26:247
46. McQuade DT, Pullen AE, Swager TM (2000) Chem Rev 100:2537
47. Kitani A, Munemura H, Takaki K, Ito S (1997) Synth Met 84:101
48. Kitani A, Munemura H, Yamashita T, Ito S (1999) Synth Met 102:1173
49. Kitani A, Munemura H, Ito S (2003) Synth Met 135–136:413
50. Tirkeş S, Cihaner A, Önal AM (2007) Polym Int 56:1040
51. Ibrahim AA, Matsumoto M, Miyahara Y, Izumi K, Suenaga M, Shimizu N, Takahiko I (1998) J Heterocycl Chem 35:209
52. Wen TC, Huang LM, Gopalan A (2001) Electrochim Acta 46:2463
53. Wu KH, Lai YS, Shih CC, Wang GP, Yang CC (2008) Polym Compos 29:902
54. Krinichnyi VI, Tokarev SV, Roth H-K, Schrödner M, Wessling B (2006) Synth Met 156:1368
55. Langer JJ, Krzyminiewski R, Kruczynski Z, Gibinski T, Czajkowski I, Framski G (2001) Synth Met 122:359
56. Shah AA, Holze R (2006) Electrochim Acta 52:1374
57. Shreepathi S, Holze R (2005) Chem Mater 17:4078
58. Dominis AJ, Spinks GM, Kane-Maguire LAP, Wallace GG (2002) Synth Met 129:165
59. Min Y, Xia Y, MacDiarmid AG, Epstein AJ (1995) Synth Met 69:159
60. Shreepathi S, Holze R (2005) Chem Mater 17:4078
61. Wen T-C, Huang L-M, Gopalan A (2001) Synth Met 123:451
62. Gupta MC, Umare SS (1992) Macromolecules 25:138
63. Mott NF, Davis EA (1971) Electronic processes in non-crystalline materials. Clarendon Press, Oxford
64. Ghosh M, Barman A, Meikap AK, De SK, Chatterjee S (1999) Phys Lett A 260:138
65. Sarkar A, Ghosh P, Meikap AK, Chattopadhyay SK, Chatterjee SK, Ghosh M (2007) Solid State Commun 143:358
66. Singh R, Tandon RP, Singh GS, Chandra S (1992) Philos Mag B 66:285
67. Singh R, Narula AK (1997) J Appl Phys 82:4362